Int. J. Environ. Sci. Technol. (2014) 11:1669–1678
DOI 10.1007/s13762-013-0318-9

ORIGINAL PAPER

A novel approach for textile dye degradation by zinc, iron–doped tin oxide/titanium moving anode

A. Vignesh · A. S. Siddarth · O. S. Gokul · B. R. Babu

Received: 15 October 2012 / Revised: 1 March 2013 / Accepted: 30 April 2013 / Published online: 25 May 2013

Abstract The present contribution reports a moving iron (Fe), zinc (Zn)–doped tin oxide/titanium (SnO_2/Ti) anode-based system designed and operated for the electro-oxidation of methyl orange dye effluent. Electrochemical oxidation of the dye was carried out at a current density of 1.8 A/dm^2 for 120 min. Similar experiments were repeated with pure SnO_2-based static and moving anode-based systems and the Fe, Zn-doped SnO_2 static anode-based electro-oxidation system. Post oxidation, the surface of the electrodes was critically examined by scanning electron microscopy. Dye samples were analysed at regular intervals during the electro-oxidation process by chemical oxygen demand and colour removal measurements and characterized by UV–Vis spectroscopy and Fourier transform infrared spectroscopy at the end of the oxidation process. The obtained results elucidate the superiority of Fe, Zn-doped SnO_2/Ti moving anode-based system for methyl orange dye effluent electro-oxidation. The moving anode prevents passive layer formation and decreases polarization resistance. Doping of Fe and Zn provides the anode-enhanced mechanical strength and electrocatalytic activity. The combined effects of axial anode movement and doping are responsible for improved performance of the moving anode system reported in this contribution.

Keywords Electrochemical treatment · SnO_2-doped electrodes · Methyl orange · Chemical oxygen demand (COD) · Scanning electron microscopy (SEM) · Fourier Transform infrared spectroscopy (FT-IR)

Introduction

The degradation of the industrial dye by electrochemical oxidation has recently emerged as a novel technology due to its simplicity and enhanced efficiency over other methods (Raghu et al. 2009). They provide better results with regard to energy efficiency, versatility, cost-effectiveness, time and chemical stability. Several reports explain the high efficiency of electrodes containing oxides of noble metals such as Ru and Ir over Ti substrates (Raghu and Basha 2007). Efforts have been taken for replacing them with transition metal oxides such as lead oxide (PbO_2), SnO_2 and antimony trioxide (Sb_2O_3) (Watts et al. 2008).

Ti/SnO_2 and Ti/PbO_2 are dimensionally stable anodes (DSA), which have higher oxygen evolution potentials than titanium/ruthenium oxide (Ti/RuO_2) (Babu et al. 2009) and titanium/iridium oxide (Ti/IrO_2) electrodes. Yet another point to be noted is that SnO_2 is more stable and non-toxic than PbO_2 (Kong et al. 2007). Ex-situ studies reveal that generation of highly reactive free hydroxyl radicals removes organic pollutants (Rodrígueza et al. 2009). SnO_2 is an important catalytic material used in a wide spectrum of areas such as gas sensors, photovoltaic and electrovoltaic systems and degradation of industrial and textile dyes. The Ti/SnO_2 anode promises a longer life due to its higher stability and capability for repeated use (Watts et al. 2008). It has been reported to enhance the rate of photocatalytic degradation of textile azo dyes (Vinodgopal and Kamat 2002). Better results have also been observed when certain amount of antimony (Sb) is doped into Ti/SnO_2 electrodes (Kong et al. 2007). The concentration of Sb plays a major role in delivering good performance. For Ti/SnO_2–Sb_2O_5 anode, 5 % of Sb dopant is an optimum concentration for electro-oxidation of 4-chlorophenol (Watts et al. 2008). Addition of Ni onto TiO_2/SnO_2–Sb electrode yields

---

A. Vignesh · A. S. Siddarth · O. S. Gokul · B. R. Babu (✉)
Pollution Control Division, CSIR—Central Electrochemical Research Institute, Karaikudi 630006, Tamil Nadu, India
e-mail: brbabu2011@gmail.com

satisfactory results (Shekarchizade and Amini 2011). Macroporous Sb-doped SnO_2/TiO_2 nanotube electrodes have successfully been synthesized and found to display superior performance as a catalyst with regard to decreasing the toxicity of p-nitrophenol (Chai et al. 2011). Hence, Sb is regarded as best suitable dopant on TiO_2/SnO_2. However, the search for an alternative material has been of great interest to many researchers. It is a proven fact that Ti/SnO_2 electrodes can be improved by doping with fluorine (F) (Elangovan and Ramamurthi 2005), platinum (Pt) (Li and Li 2002), nickel (Ni) (Borodzínski and Lasia 1994), Fe (Carneiro et al. 2005) and various metals (Yang et al. 2012).

Transition metal doping induces specific properties on TiO_2/SnO_2 electrode. Enhancements in mechanical strength, photocatalytic activity (Chai et al. 2011), electrocatalytic activity (He and Mho 2004; Zaleska 2008), dye degradation rate and total organic carbon (TOC) removal rate (Carneiro et al. 2005) have been reported on SnO_2 electrodes doped with Fe. There was a threefold increase in the degradation of phenolic compounds on Fe(III)-doped Sb–SnO_2 electrode (Carneiro et al. 2005). Moreover, Fe^{2+} produces hydroxyl radical, which has a strong affinity for organic bond rupture (Babu et al. 2010). Hence, Fe can be considered as a better dopant. Zn doping prevents the electrode from degradation under sunlight (Yang et al. 2012), provides environmental protection and makes the electrode available for commercial use. Moreover, ionic radius of Zn^{2+} is similar to that of Sn^{4+}, giving rise to more oxygen vacancies (He and Mho 2004). Zn also increases electrocatalytic activity (Sun et al. 2012) and efficiency of phenol degradation (Pawar and Nimbalkar 2012).

The aim of this work is to fabricate Fe (Dyntu et al. 2009; Tsipis et al. 2011) (to improve mechanical strength), Zn (to enhance electrocatalytic activity)-doped SnO_2 on Ti mesh substrate for degradation of methyl orange, a common textile dye. In the present contribution, we have placed special emphasis on electro-oxidative dye degradation studies in systems containing a moving anode and recirculating the effluent. A moving anode is employed in order to increase the overall efficiency of electro-oxidation by enhancing electrode–solution contact through the prevention of passive layer formation on the electrode surface. The absence of a passive layer also contributes to increased electrode conductivity and a decrease in polarization resistance. Yet another advantage of moving electrode systems is that electrode life is enhanced as a consequence of reduced pitting damage due to absence of passive layer.

The Fe, Zn-doped SnO_2/Ti anode was reciprocated by using a camshaft motor, and the methyl orange dye effluent was continuously re-circulated through the cell. In the present report, the superiority of this system is demonstrated by comparative analysis with pure SnO_2/Ti static and moving electrode systems and the static Fe, Zn-doped SnO_2/Ti anode-based system. It is the combined effects of doping and anode motion that makes the Fe, Zn-doped SnO_2/Ti moving anode methyl orange electro-oxidation system truly stand a class apart. This fact can be construed from the results reported further in this contribution, which are comparable with the commonly reported Ti/SnO_2–Sb and doped SnO_2/Ti anodes (Kong et al. 2007; Raghu et al. 2009; Watts et al. 2008; Zhao et al. 2009).

This contribution is the product of research work undertaken by our group at the Electrochemical Pollution Control Division of CSIR-Central Electrochemical Research Institute, Karaikudi, TN, India, during the months of March–August 2012.

Materials and methods

Materials

All chemicals employed were of the “AR” grade, and purchased from Merck India Ltd. Laboratory equipments had been calibrated with due accordance to accepted standards, and double deionized water was used while conducting all experiments. The methyl orange dye samples were collected from a textile industry located at Tirupur, Tamil Nadu, India.

Electrode preparation

Type 1: Tin oxide electrode

0.35 gpl of tin chloride pentahydrate ($SnCl_4{\cdot}5H_2O$) was dissolved in a solution of ethanol, and hydrochloric acid (HCl) was added for pH maintenance. The solution was placed under continuous stirring for a time period of 1 h and then coated over a titanium mesh by brush coating. Sintering of the coated electrode was carried out at 650 °C for 10 min. The same procedure was repeated for about 10 times in order to obtain a desired thickness.

Type 2: Fe–Zn-doped tin oxide electrode

Preparation of doped tin oxide electrode was carried out by the same procedure that had been elucidated in Type 1. The solution was prepared by dissolving 0.28 gpl of $SnCl_4{\cdot}5H_2O$, 0.054 gpl of Ferric chloride hexahydrate ($FeCl_3{\cdot}6H_2O$) and 0.04 gpl of zinc chloride ($ZnCl_2$), with HCl addition for pH maintenance.

The prepared electrodes were characterized by X-ray diffraction (XRD) and scanning electron microscopy (SEM) was used to study the surface morphology of the anodes post treatment.

Electro-oxidation (EO) set-up

Static electrode arrangement

EO of methyl orange dye was carried out by employing the prepared electrodes as anode and stainless steel as cathode. EO was carried out for a period of 120 min at constant current density of 1.8 A/dm^2 under static electrode conditions. The methyl orange effluent was circulated at a flow rate of 30 ml/min. 0.4 g of NaCl was added to the dye in order to facilitate conductivity.

Moving electrode arrangements

The basic electrolytic set-up is same as that discussed in previous section. The prepared electrode was fixed to a camshaft rotating at a constant rate of 10 rpm, and the electrolyte was recirculated at constant flow rate. Figure 1 depicts the experimental set-up for a typical moving anode electro-oxidation system.

The degradation of dye was monitored by colour removal measurements and reduction in COD. FT-IR and UV–Vis spectroscopic analyses had been conducted to detect optical and functional group modifications in the dye as a result of electro-oxidation. SEM was used to characterize the morphology of used anodes in static and moving conditions.

Structural and physico-chemical characterization

UV–Visible spectrum

UV–Visible spectrum was used to monitor the de-colorization of methyl orange dye at various time intervals. The spectra had been recorded by UV Spectroquant 50 with a wavelength of 240 nm. The plots reported had been recorded after electrochemical oxidation for a time period of 120 min.

FT-IR analysis

The electrolytic breakdown of organic functional groups in methyl orange dye was monitored by FT-IR spectrum along the mid-IR region of 400–4,000 cm^{-1}. The sample had directly been placed on the KBr crystal, and recording of spectrum was carried out through transmittance mode.

Crystal phase and morphology

The crystal phase of electrodes under study had been studied by XRD measurements. A computer controlled XRD-system, JEOL Model: JPX-8030 with CuK radiation (Ni filtered = 13,418 Å) at the range of 40 kV, 20 A was used for recording the XRD pattern. Identification of pertinent peaks was carried out using the standard data provided by the International Centre for Diffraction Data (ICDD).

The anode surface morphology was imaged using a SEM BRUKER TESCAN. The SEM images provide valuable data on dimensional stability of anodes in static and moving electrode electro-oxidation systems.

Chemical oxygen demand (COD) measurements

Measurements of COD in the dye were made at regular time intervals by acid solution precipitation method. A predetermined quantity of solution was blended with COD acid and potassium dichromate solutions. The mixture was

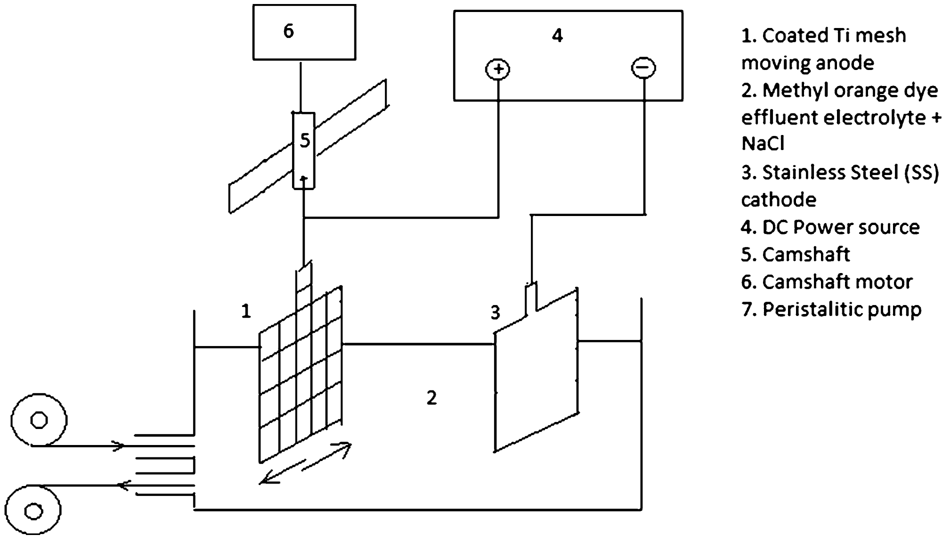

Fig. 1 Schematic representation of moving electrode set-up for methyl orange electro-oxidation

placed in a COD digester (Spectroquant TR 420, Merck) at 148 °C for 120 min. It was then titrated against ferrous ammonium sulphate (FAS) solution using ferroin as the indicator. A change in colour from red to brown indicated the end point. The COD is then calculated as follows:

$$\mathrm{COD\ (mg/L)} = (V_1 - V_2) \times 8{,}000 \times N / X$$

where V_1 titre value in mL of blank sample (water), V_2 titre value in mL of methyl orange sample under study, N normality of FAS, X volume of sample.

Electrochemical impedance spectroscopy (EIS)

The electrochemical behaviour of pure and Fe, Zn-doped SnO_2/Ti mesh anodes was studied by EIS. The working electrode employed for impedance studies consisted of the anode mesh under study, with an exposure area of 1 cm^2 in effluent solution containing 1 g/l NaCl as supporting electrolyte. Saturated calomel electrode (SCE) was used as the reference electrode, and platinum was used as the counter electrode. Impedance studies were performed using an electrochemical analyser IM6. After the attainment of steady state, an AC signal of amplitude 3 mV at 2.5 V was applied, and impedance values were measured for frequencies ranging from 100 kHz to 10 mHz. Nyquist plots were plotted for the measurement of R_s and R_p values.

Results and discussion

UV–Visible spectroscopy

UV–Visible spectrophotometer has been employed to measure the changes in absorbance characteristics of dye effluent over a large wavelength interval during the electrochemical oxidization process. Plot M in Fig. 2 is the UV–Vis spectrum of raw dye effluent. The plots (a) and (c) of Fig. 2 show the recorded spectra of dye effluents oxidized with pure and Fe, Zn-doped SnO_2 coated Ti electrodes under static electrode conditions, and plots (b) and (d) are the spectra for the moving electrode system.

Methyl orange may be yellow or reddish orange in colour depending on the presence of substituted azobenzene or azobenzene functional groups. Two broad absorbance peaks in the visible region at 390 and 600 nm can be observed from the UV–Vis spectrum. The absorbance peak at 390 nm corresponds to the substituted azobenzene group, and that at 600 nm is typical of azobenzene group.

There is a gradual decrease in peak absorbance values as electro-oxidation proceeds with time. Such an observation indicates the oxidation of organic functional groups, resulting in colour removal. Thus, electrochemical oxidation has proved to be an efficient means of colour reduction in the dye effluent.

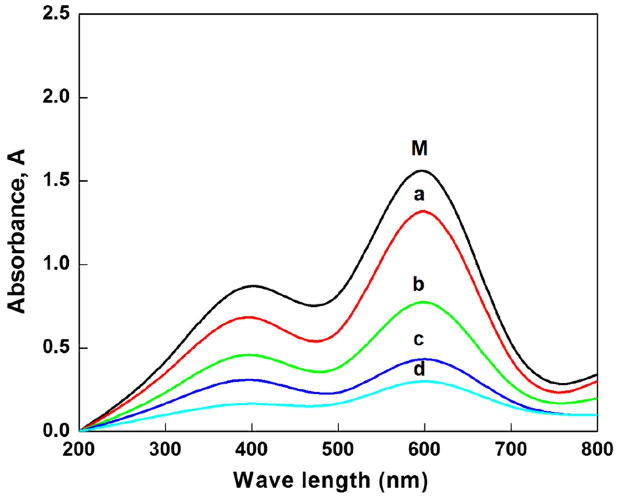

Fig. 2 UV visible spectra of methyl orange dye after electro-oxidation for 120 min at 1.8 A/dm^2 using *a* pure SnO_2/Ti static anode, *b* pure SnO_2/Ti moving anode, *c* Fe, Zn-doped SnO_2/Ti static anode, *d* Fe, Zn-doped SnO_2/Ti moving anode. *M* UV–Visible spectra of raw methyl orange effluent

From Fig. 2, a maximum fall in peak absorbance can be observed when electro-oxidation is carried out with moving Fe, Zn-doped SnO_2 electrodes (d). This offers a clear indication of the superiority of moving electrode systems with regard to methyl orange electro-oxidation. It can also be seen from the figure that when compared with pure SnO_2/Ti electrode-based systems, there is a greater decrease in peak absorbance values for Fe, Zn-doped SnO_2/Ti electrodes. This may be attributed to greater electrocatalytic activity of SnO_2 doped with Fe and Zn.

The percentage colour removal at various time intervals during electro-oxidation can be calculated from the change in maximum wavelength absorbance peak values at each time interval. A general formula used for the calculation of percentage colour removal is given below

$$\%\ \mathrm{Color\ removal} = 100 \times \{(A_0 - A_t)/A_t\}$$

where A_0 maximum wavelength peak absorbance value prior to electro-oxidation, A_t maximum wavelength peak absorbance value after electro-oxidation for a time period t.

Figure 3 is a plot of percentage de-colorization versus time for static and moving electrode-based electro-oxidation systems. The absorbance peak value at 390 nm was used for colour removal studies. In static systems, it is observed that Fe–Zn-doped SnO_2 coated Ti anodes show higher rates of colour removal than bare SnO_2/Ti anodes. It can be noticed from the figure that a maximum of 97 % colour removal is observed in moving electrode Fe–Zn-doped SnO_2 coated Ti anode-based systems at the end of 120 min. This system also exhibits a higher overall trend with regard to the rate of dye de-colorization, when compared to the other static systems under study. The efficient performance of moving electrode system can be explained on the basis of decreased polarization resistance. It may also be attributed to greater electrode–solution contact, and absence of anodic passivation as a result of continuous axial movement in solution.

Chemical oxygen demand (COD)

Figure 4 is a plot of percentage COD reduction at various time intervals in static and moving electrode systems. A maximum COD reduction of 89.7 % can be noticed in the Fe–Zn-doped SnO_2/Ti moving electrode-based system at the end of 120 min. The static Fe, Zn-doped SnO_2-based system exhibits a maximum COD reduction of 88.5 %. A COD reduction of 85.8 % is observed in the pure SnO_2/Ti moving electrode-based system, and the static system exhibits an even lower COD reduction of 82.9 %. As COD is amount of oxygen required by organic compounds present in the effluent to get oxidized, a reduced COD facilitates easier oxidation of organic compounds, culminating in functional group modification and colour removal.

Table 1 provides the physico-chemical characteristics of textile dye effluent prior to and post electro-oxidation by various anode systems.

FT-IR spectroscopy

Figure 5 depicts the FT-IR spectra of methyl orange post electro-oxidation with different electrode systems. The broad peak at 3,420.06 cm^{-1} corresponds to primary O–H stretching vibrations of hydroxyl functional group, and that at 660.02 cm^{-1} may be attributed to out of plane bending of aromatic O–H groups. C=O stretching vibrations of phenolic hydroxyl groups have led to the formation of a minor peak at 1,127.05 cm^{-1}. The sharp peak at 1,536.92 has resulted from vibrations of N–H group.

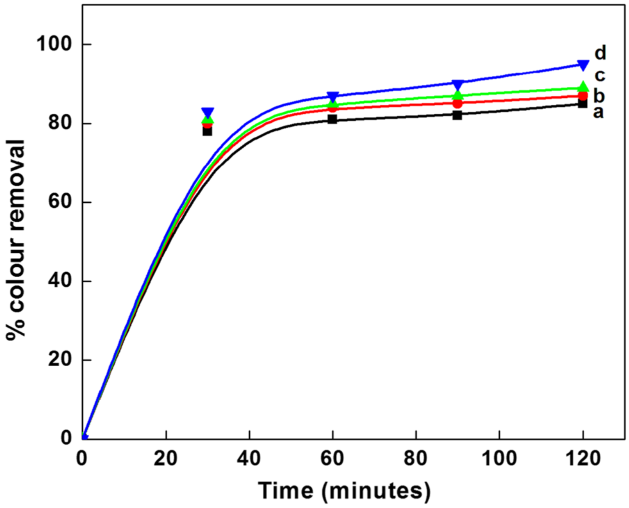

Fig. 3 *Colour* removal measurements at 390 nm peak absorbance for electro-oxidation using *a* pure SnO_2/Ti static anode, *b* pure SnO_2/Ti moving anode, *c* Fe, Zn-doped SnO_2/Ti static anode, *d* Fe, Zn-doped SnO_2/Ti moving anode

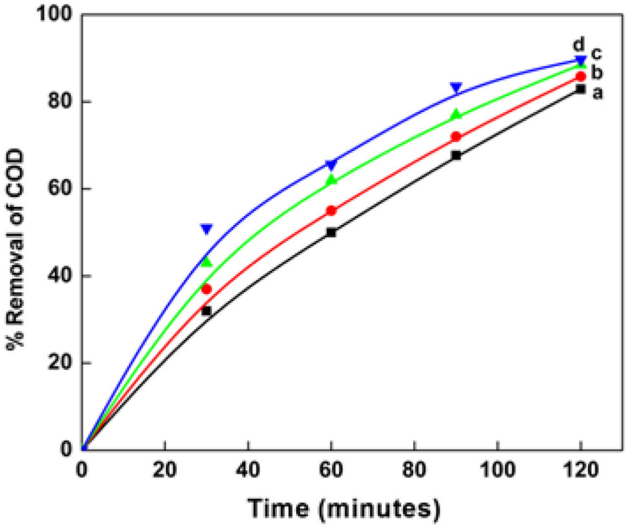

Fig. 4 Chemical oxygen demand (COD) measurements for electro-oxidation using *a* pure SnO_2/Ti static anode, *b* pure SnO_2/Ti moving anode, *c* Fe, Zn-doped SnO_2/Ti static anode, *d* Fe, Zn-doped SnO_2/Ti moving anode

All functional group peaks are visible in the pure SnO_2/Ti static electrode-based system (a), whereas a significant reduction in peak transmission intensity is seen in the Fe, Zn-doped SnO_2/Ti static electrode-based system (b).

Curve (c) is the spectra of methyl orange oxidized with pure SnO_2/Ti moving electrode-based system. When compared to the static system, a decrease in the intensity of functional group vibrations is clearly visible. The electro-oxidation of methyl orange using Fe, Zn SnO_2/Ti moving electrode-based system is shown in the curve (a). It can be seen that vibrations due to aromatic groups and N–H groups are completely diminished, and the O–H stretching vibrations are reduced substantially. Such observations prove the effectiveness of moving electrode-based system with regard to methyl orange electro-oxidation.

Hence, it can be seen that observations from UV–Vis and FT-IR studies co-relate well with obtained results on COD reduction.

X-ray diffraction studies

Figure 6a is the XRD spectra of pure SnO_2/Ti electrode. The peaks at 28.15°, 54°, 56° and 77° correspond to the crystal planes of SnO_2. The residual peaks at 39°, 40°, 63° and 71° belong to Ti mesh base.

Table 1 Physico-chemical characteristics of textile dye effluent

S. no.	Parameter	Raw effluent	After electro-oxidation with pure SnO_2/Ti static anode	After electro-oxidation with pure SnO_2/Ti moving anode	After electro-oxidation with Fe, Zn-doped SnO_2/Ti static anode	After electro-oxidation with Fe, Zn-doped SnO_2/Ti moving anode
1	COD (mg/L)	1,555	265	220.2	178.6	160
2	pH	6.5	6.2	5.8	5.5	5.2
3	BOD (mg/L)	265	121	104	117	92
4	Suspended solids (mg/L)	310	302	294	285	276
5	Conductivity (μmho/cm)	2,650	2,853	2,967	3,018	3,094

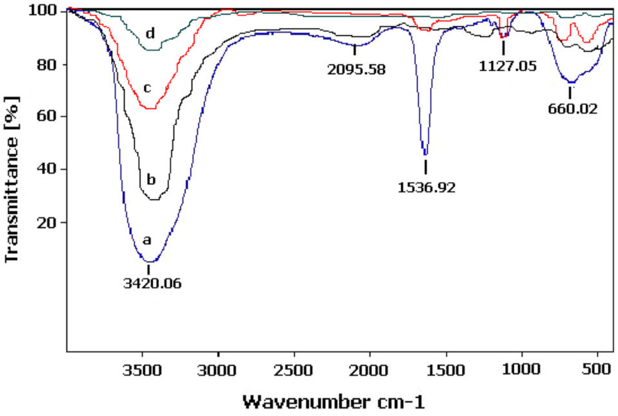

Fig. 5 FT-IR spectra of methyl orange dye post electro-oxidation using *a* pure SnO_2/Ti static anode, *b* pure SnO_2/Ti moving anode, *c* Fe, Zn-doped SnO_2/Ti static anode, *d* Fe, Zn-doped SnO_2/Ti moving anode

The XRD spectra of Fe, Zn-doped SnO_2/Ti electrode are shown in Fig. 6b. Two additional peaks are visible at 36.01° and 44.10°, due to the diffraction caused by Zn and Fe crystal planes, respectively. This indicates the inclusion of Fe and Zn impurities into the crystal lattice of SnO_2, rendering it enhanced mechanical stability and greater electrocatalytic activity with regard to phenol degradation.

The indexing of XRD had been carried out with reference to the standard data provided by ICDD.

Scanning electron microscopy

The surface morphology of anodes had been critically imaged by SEM. Figure 7a, d is the SEM images of pure SnO_2/Ti and Fe, Zn-doped SnO_2/Ti anodes prior to electro-oxidation.

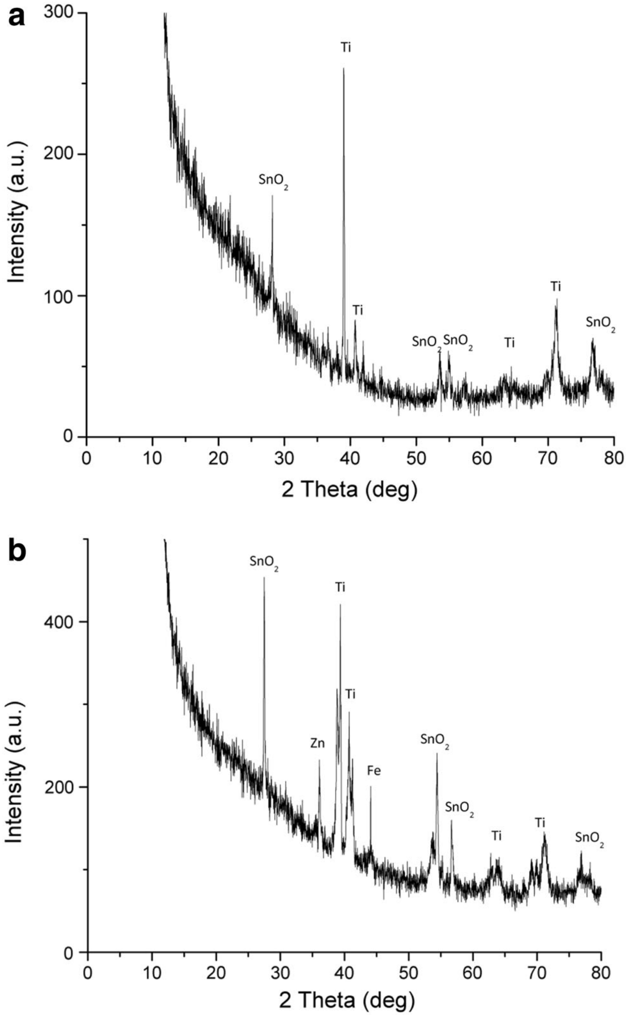

Fig. 6 **a** X-ray diffraction (XRD) pattern of pure SnO_2/Ti anode prior to use for electro-oxidation. **b** X-ray diffraction (XRD) pattern of Fe, Zn-doped SnO_2/Ti anode prior to use for electro-oxidation

Figure 7b is the SEM image of spent pure SnO_2/Ti static anode, showing a voluminous amount of surface cracks and aberrations. This may be attributed to anode wear as a result of passive layer formation and partial breakdown, resulting in regions of uneven solution concentration. A lesser number of cracks are seen in the pure SnO_2/Ti moving electrode system, as seen from Fig. 7c. Such an observation is due to the fact that axial electrode movement

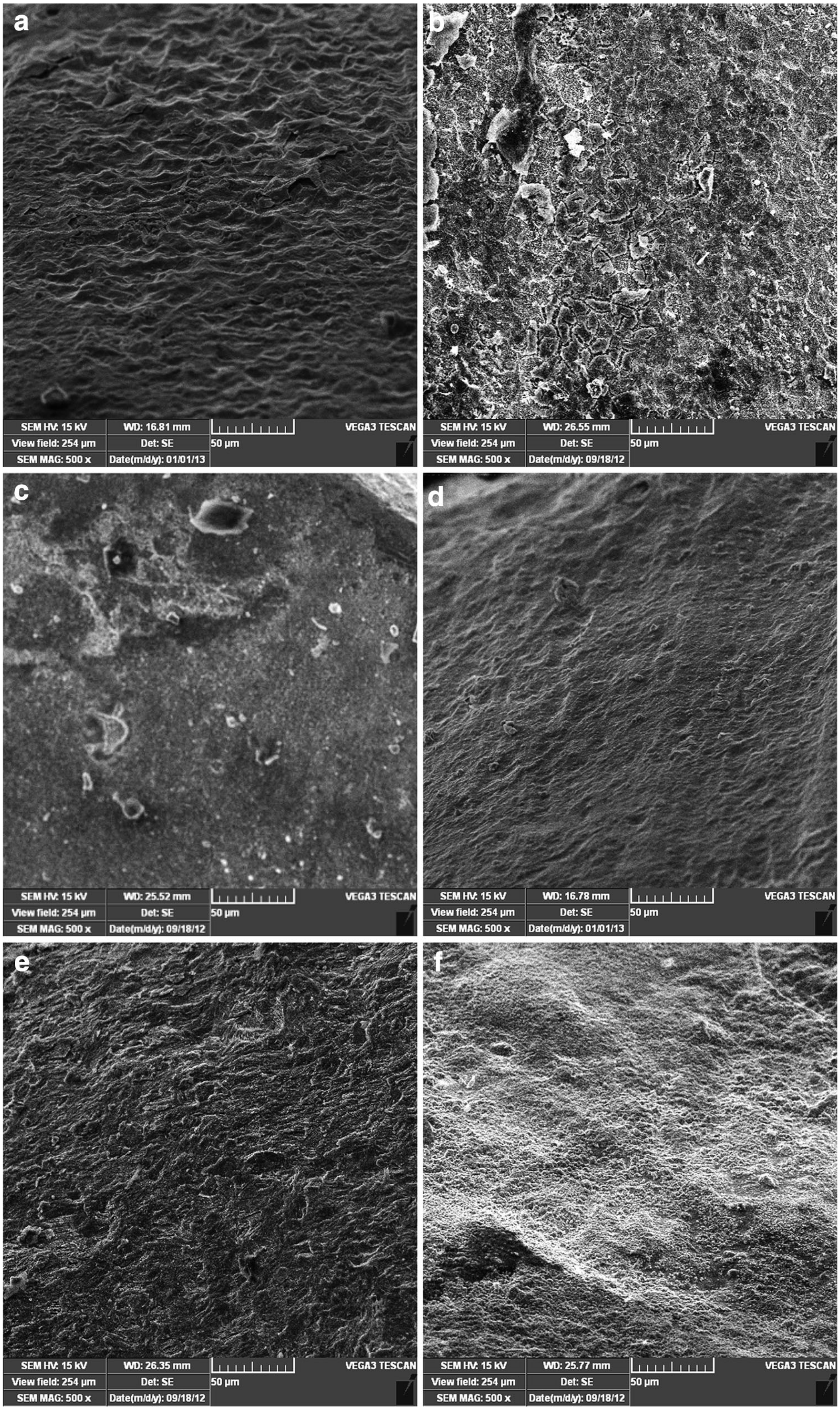

Fig. 7 **a** SEM image of pure SnO_2/Ti anode prior to electro-oxidation. **b** SEM image of pure SnO_2/Ti anode post electro-oxidation in static condition. **c** SEM image of pure SnO_2/Ti anode post electro-oxidation moving condition. **d** SEM image of Fe, Zn-doped SnO_2/Ti anode prior to electro-oxidation. **e** SEM image of Fe, Zn-doped SnO_2/Ti anode post electro-oxidation in static condition. **f** SEM image of Fe, Zn-doped SnO_2/Ti anode post electro-oxidation in moving condition

prevents the formation of passive layer on the anode surface. This phenomenon also enhances solution–electrode contact, improving overall process efficiency.

Inclusion of Fe by doping improves the mechanical strength of SnO_2/Ti anode to an enormous extent, as we may observe from Fig. 7e, the SEM image of spent Fe, Zn-doped SnO_2/Ti static anode, which has a relatively smooth surface with minimal number of cracks. The best results are observed in the Fe, Zn-doped SnO_2/Ti moving electrode-based system, which is mostly free of cracks, and relatively smooth when compared to other systems, as shown in Fig. 7f. This is attributed to the combined effects resulting from the prevention of passive layer formation and mechanical stability offered by Fe addition. Hence, we propose the Fe, Zn-doped SnO_2/Ti moving anode model as one of great promise with regard to enhanced efficiency and extended operating life.

Electrochemical impedance spectroscopy (EIS)

The Fig. 8 depicts the Nyquist plots of pure and Fe, Zn-doped SnO_2/Ti anodes in dye effluent solution, to which 1 g/L of NaCl was added. Curves a and b in the Fig. 8 are the Nyquist plots for pure SnO_2/Ti static and moving anodes, respectively, while c and d are those static and moving Fe, Zn-doped SnO_2/Ti anodes. In all four studies, the solution resistance was measured to be constant at 3.1 ohm. The polarization resistance was seen to have a maximum value of 156.4 ohm for the static SnO_2/Ti anode. There was a slight decrease in the polarization resistance to 142.3 ohm in the moving SnO_2/Ti anode. Doping of Fe and Zn renders a significant increase in surface electrocatalytic activity, resulting in a further polarization resistance decrease to 133.1 ohm. The least resistance to polarization was seen in the Fe, Zn-doped moving anode system, in which the R_p value was at 121.7 ohm. This greatly increases the rate of charge transfer on the electrode surface, resulting in superior performance with respect to the electro-oxidation of organic effluents. The low value of polarization resistance in the Fe, Zn-doped moving anode system may be attributed to the combined effects of increased electrode–solution contact and greater electrocatalytic activity, rendered by electrode movement and doping, respectively. The observations from electrochemical impedance study complement our results from colour removal, functional group removal and COD reduction data.

Electro-oxidation mechanism

The general mechanism of SnO_2-based electrodes in oxidizing pollutants has been reported elsewhere (Zhao et al. 2009). The electro-oxidative degradation of organic pollutants is initiated by splitting of water into hydroxyl radicals and subsequently, adsorption of hydroxyl radicals on the electrode surface. This is followed by the oxidation of pollutants (R) to produce intermediates that ultimately break down with the release of H_2O and CO_2 at greater radical concentrations. The combination of hydroxyl radicals may also lead to the formation of O_2 as a by-product.

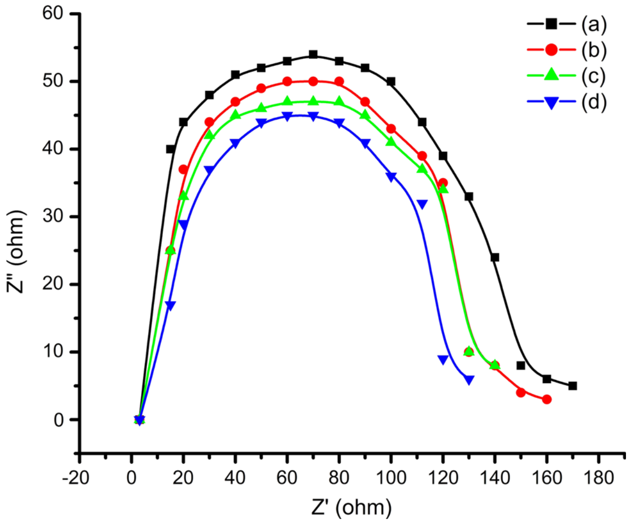

Fig. 8 Electrochemical impedance spectra. *a* Pure SnO_2/Ti static anode, *b* pure SnO_2/Ti moving anode, *c* Fe, Zn-doped SnO_2/Ti static anode, *d* Fe, Zn-doped SnO_2/Ti moving anode

$$SnO_2 + H_2O \rightarrow SnO_2(^{\cdot}OH) + H^+ + e^-$$

$$^{\cdot}OH + R \rightarrow RO + H^+$$

$$RO + H^+ \rightarrow CO_2 + H_2O$$

$$^{\cdot}OH + ^{\cdot}OH \rightarrow H_2O + 1/2\ O_2 \uparrow$$

Fe^{2+} serves as a source for hydroxyl radicals, as reported by Babu et al. (2010). Hence, the doping of Fe on SnO_2/Ti anode may increase radical concentration to a great extent, leading to the efficient degradation of organic pollutants. Moreover, doping of Fe renders greater mechanical stability (Dyntu et al. 2009), as seen from the SEM images of spent Fe, Zn-doped SnO_2/Ti anodes.

The similarity between the ionic radii of Zn^{2+} and Sn^{4+} gives rise to a greater number of oxygen vacancies (He and Mho 2004). It serves as an efficient electrocatalyst (Sun et al. 2012) for phenolic degradation in particular (Pawar and Nimbalkar 2012). Zn doping also serves to increase electrode life by preventing photodegradation (Yang et al. 2012).

The motion of electrode greatly increases electrode–solution contact, effectively leading to more efficient electro-oxidation of organic pollutants, as one may observe from the results reported. Thus, the Fe, Zn-doped SnO_2/Ti anode offers much promise as an efficient system for electrochemical effluent treatment in the future.

Conclusion

In the present experiment, pure and Fe, Zn-doped SnO_2/Ti anodes were prepared and studied under static and moving anode electro-oxidation conditions. Superior results have been obtained for the Fe, Zn-doped moving anode system for methyl orange electro-oxidation. The dye effluent COD was reduced by 89.7, and 97 % colour removal was achieved after electro-oxidation for 120 min under a constant current density of 1.8 A/dm^2. The spent anode is relatively smooth and free of cracks, as seen from SEM images. This indicates the mechanical stability of Fe, Zn-doped moving anode system under operating conditions.

The decrease in polarization resistance and possible absence of passive layer formation in moving electrode systems enhance electrode–electrolyte contact, paving way for efficient electro-oxidation. Moreover, the doping of Fe and Zn unto SnO_2 greatly increases its mechanical strength and electrocatalytic activity for phenolic degradation. Such facts may be readily co-related with the results obtained.

Scrutinizing the observed results, we conclude by stating that the Fe, Zn-doped SnO_2/Ti moving electrode system discussed in this contribution is highly cost effective when compared to conventional systems which consists of RuO_2/IrO_2 coated Ti anodes and shows great promise as a novel technology for dye effluent degradation. Future work would involve real-time dynamic computational simulations on moving electrode-based dye electro-oxidation systems, investigation of novel dopants, variation of process parameters and pilot-scale studies.

Acknowledgments The council of scientific and industrial research (CSIR), New Delhi is gratefully acknowledged for funding work on this contribution (SETCA Project No: ILP003). The authors also wish to express their gratitude to Mr. Ravi shanker, Miss. S. Krithika and Mrs. Panchali of CECRI's Central Instrumentation Facility (CIF) for their assistance in the utilization of analytical facilities vital in accurate interpretation of results.

References

Babu BR, Venkatesan P, Kanimozhi R, Basha CA (2009) Removal of pharmaceuticals from wastewater by electrochemical oxidation using cylindrical flow reactor and optimization treatment conditions. J Environ Sci Health Part A Environ Sci Eng 44:985–994

Babu BR, Meera KS, Venkatesan P, Sunandha D (2010) Removal of fatty acids from palm oil effluent by combined electro-fenton and biological oxidation process. Water Air Soil Pollut 211:203–210

Borodzínski JJ, Lasia A (1994) Electrocatalytic property of doped nickel boride based electrodes for the Hydrogen evolution reaction. J Appl Electrochem 24(12):1267–1275

Carneiro JO, Teixeira V, Portinha A, Dupak L, Magalhaes A, Coutinho P (2005) Study of the deposition parameters and Fe-dopant effect in the photocatalytic activity of TiO_2 films prepared by DC reactive magnetron sputtering. Coden Vac 78(1):37–46

Chai S, Zhao G, Li P, Lei Y, Zhang YN, Li D (2011) Novel sieve-like SnO_2/TiO_2 nanotubes with integrated photoelectrocatalysis: fabrication and application for efficient toxicity elimination of nitrophenol wastewater. J Phys Chem C 115(37):18261–18269

Dyntu M, Meglei D, Donu S, Rusu A (2009) Mechanical properties of iron doped bismuth microwire in glass isolation. MJPS 8(N2):231–233

Elangovan E, Ramamurthi K (2005) Studies on micro-structural and electrical properties of spray-deposited fluorine-doped tin oxide thin films from low-cost precursor. Thin Solid Films 476(2):231–236

He D, Mho SI (2004) Electrocatalytic reaction of phenolic compounds at ferric ion co-doped SnO_2:Sb^{5+} electrodes. J Electroanal Chem 568(1):19–27

Kong JT, Shi SY, Zhu XP, Ni JR (2007) Effect of Sb dopant amount on the structure and electrocatalytic capability of Ti/Sb–SnO_2 electrodes in the oxidation of 4-chlorophenol. J Environ Sci 19(11):1380–1386

Li XZ, Li FB (2002) The enhancement of photodegradation efficiency using Pt–TiO_2 catalyst. Chemosphere 48:1103–1111

Pawar MJ, Nimbalkar VB (2012) Synthesis and phenol degradation activity of Zn and Cr doped TiO_2 Nanoparticles. Res J Chem Sci 2(1):32–37

Raghu S, Basha CA (2007) Electrochemical treatment of Procion Black 5B using cylindrical flow reactor—a pilot plant study. J Hazard Mater 139(2):381–390

Raghu S, Lee CW, Chellammal S, Palanichamy S, Basha CA (2009) Evaluation of electrochemical oxidation techniques for degradation of dye effluents—a comparative approach. J Hazard Mater 171(1–3):748–754

Rodrígueza MV, Ramíreza AH, Hernándeza JMP, Bandalab ER, Alfaro MAQ (2009) Enhancing the electrochemical oxidation of acid-yellow 36 azo dye using boron-doped diamond electrodes by addition of ferrous ion. J Hazard Mater 167(1–3):1226–1230

Shekarchizade H, Amini MK (2011) Effect of elemental composition on the structure, electrochemical properties, and ozone production activity of Ti/SnO_2–Sb–Ni electrodes prepared by thermal pyrolysis method. Int J Electrochem. doi:10.4061/2011/240837

Sun P, You L, Sun Y, Chen N, Li X, Sun H, Ma J, Lu G (2012) Novel Zn-doped SnO_2 hierarchical architectures: synthesis characterization, and gas sensing properties. CrystEngComm 14(5):1701–1708

Tsipis EV, Waerenborgh JC, Kharton VV (2011) Surface states and stability of Fe containing perovskite electrodes for SOFCs/SOECs by conversion-electron Mössbauer spectroscopy. Electrochem Commun 13:685–688

Vinodgopal K, Kamat PV (2002) Enhanced rates of photocatalytic degradation of an azo dye using SnO_2/TiO_2 coupled semiconductor thin films. Environ Sci Technol 29(3):841–845

Watts RJ, Wyeth MS, Finn DD, Teel AL (2008) Optimization of Ti/SnO_2–Sb_2O_5 anode preparation for electrochemical oxidation of organic contaminants in water and wastewater. J Appl Electrochem 38(1):31–37

Yang SY, Choo YS, Kim S (2012) Boosting the electrocatalytic activities of SnO_2 electrodes for remediation of aqueous pollutants by doping with various metals. Appl Catal B Environ 111:317–325

Zaleska A (2008) Doped-TiO_2: a review. Recent Pat Eng 2:157–164

Zhao GH, Cui X, Liu MC (2009) Electrochemical degradation of refractory pollutant using a novel microstructured TiO_2 nanotubes/Sb-doped SnO_2 electrode. Environ Sci Technol 43:1480